scientific reports

OPEN

A metric for quantifying adaptation to successive disruptions

Floris van Steijn[1]✉, Nazli Yonca Aydin[1], Neelke Doorn[1] & Tina Comes[1,2]

Complex systems face a myriad of stresses and shocks. The ability of complex systems to deal with such shocks is often expressed in terms of the system's resilience. Although resilience is conventionally conceptualised as recovery from a single shock or disruption, in reality, systems often face a sequence of successive shocks, as is the case for earthquake aftershocks or epidemic waves. A system's ability to handle such a sequence of disruptions depends on its capacity to learn from preceding events. To capture adaptation and learning as transformative aspects of resilience, new approaches to account for performance changes across successive disruptions are needed. This paper addresses this gap by developing and empirically testing a novel, performance-based method to quantify adaptation to successive shocks, thereby contributing to the broader discussion on adaptation and resilience. We use the COVID-19 pandemic as a case study which was characterised by multiple waves across different countries and contexts, making it an ideal case to test our theoretical model. We use open-source data from Our World in Data, ranging from 2020 to 2023, and consider every COVID-19 wave as a disruption. Individual waves are identified by fitting mixtures of skew-normal curves to COVID-19 fatality time series, and a performance-based resilience metric, called the Total Performance Loss (TPL), is computed for each wave. Adaptation across successive waves is modelled using an exponential, learning-based metric that captures whether system performance improves or deteriorates over time. The results show that many countries initially showed maladaptive behaviour but adapted in later pandemic waves. The proposed methodology makes adaptation to successive disruptions measurable, and enables systematic comparison of how systems learn, and unlearn over time, which is an essential step towards understanding and improving responses to future crises.

Keywords Adaptation, Measuring resilience, Successive disruptions, COVID-19

Complex systems are frequently exposed to a wide range of disruptions. When these systems are responsible for providing critical functions that significantly affect people's lives, it is crucial that they are capable of effectively dealing with these disruptions. In other words, it is crucial that they are resilient.

The conventional view that portrays resilience as a system's capacity to respond and recover from an isolated disruption is becoming increasingly inadequate in this context[1]. Today's poly-crises, ranging from COVID-19 to increasing geopolitical conflict and climate change, have exposed the limitations of the existing resilience frameworks and assessment methodologies. Today's disruptions are unavoidably entangled and interwoven as they co-occur, overlap, and persist over prolonged periods of time. Traditional methods to measure resilience are not able to describe and analyse this complexity[2]. Therefore, it is necessary to develop a method that more accurately captures the dynamic and interdependent nature of the current disruptions[1].

Within the context of continuously evolving and dynamic crises, adaptation emerges as a critical component for understanding resilience and enabling a system to achieve a resilient response. Rooted in the definition of social-ecological resilience[3], adaptation is defined as the capacity of a system to adjust in response to changing conditions, thus maintaining or even improving its functionality in the face of disruptions. The concept of adaptation focuses on the ability of a system to learn from disruptions and to modify its responses over time. Positioning adaptation as a central component of resilience assessment allows for a deeper understanding of the long-term behavioural dynamics of systems under crisis, which is essential for informing policy development and strategic planning in the context of multiple and overlapping (i.e., poly-)crises.

In general terms, resilience assessment provides the means to evaluate the degree to which a system can withstand or how rapidly it can recover from disruptions, thus providing the much-needed empirical grounding for strategic decisions[4]. In current literature, resilience assessment falls broadly into two realms: (a) indicator-based assessments provide a snapshot of a system's condition at a particular point in time to model resilience

[1]Faculty of Technology, Policy and Management, TU Delft, Delft, The Netherlands. [2]Institute for the Protection of Terrestrial Infrastructures, German Aerospace Center, Sankt Augustin, Germany. ✉email: F.P.vanSteijn@tudelft.nl

prior to a disruption[5], (b) performance-based assessments capture how and how rapidly a system recovers, either based on empirical data or model-based simulations[6].

Despite the crucial role of adaptation in the context of contemporary poly-crises, much of the current literature continues to focus on isolated disruptions rather than evaluating the extent to which systems can learn and enhance their adaptive capacities and responses over time[7]. Consequently, resilience metrics often remain focused on isolated disruptions, instead of learning and improving capacities and responses over time. This emphasis results in a neglect of the adaptive capacity of systems in resilience policy, a crucial factor when considering long-term resilience.

We aim to address this gap by focusing on measuring adaptation to successive disruptions as a core component of measuring resilience. The underlying premise is that systems may improve or deteriorate their response capabilities over time when they are exposed to successive disruptions. Our adaptation assessment approach contains a novel adaptation metric that aims to capture these patterns of learning and improvement, or, conversely, patterns of decline. By measuring adaptation across a sequence of events, our approach aims to provide insights into the evolving response behaviours of systems over extended periods, thereby facilitating the development of adaptive strategies for resilience.

To illustrate the analytical potential and practical implications of the novel metric, we use the COVID-19 pandemic as a case study. The COVID-19 pandemic is an ideal case study since its multiple waves constitute successive disruptions, and the pandemic is well-documented on a global scale.

Our contribution is thus twofold. First, we propose a novel method for modelling adaptation and the resulting metric that quantifies adaptation to successive disruptions. This method seeks to foster a more nuanced understanding of dynamic system behaviour under prolonged stresses and disruptions. Second, we use our metric to analyse COVID-19 responses globally. This method allows us to identify inter-country variations in adaptation patterns and analyse distinct pathways to resilience across countries. The case study thus provides empirical insights into the patterns of adaptation capacity during a global crisis.

The remainder of the paper is structured as follows: in the *Background*, we provide the theoretical and analytical context on resilience measurement and adaptation. From there, we present the methodology for the adaptation metric in the *Quantifying Adaptation* section, and describe the application of this methodology to the case study in *COVID-19 Case Study: Measuring Adaptation of 185 Countries and Territories*. The *Results* section provides the results of the case study, and in the *Discussion*, these results and the limitations are discussed. We conclude the paper in the *Conclusion* section.

Background

Quantifying the resilience of single disruptions

Performance-based resilience assessment methods start from identifying a set of key performance indicators that adequately represent and measure the essential or desired functions that the system is meant to uphold. For example, the performance of a water distribution system can be measured in terms of the number of customers served[8,9], the performance of a mobility system can be measured by the percentage of people with access to critical locations[10], and the performance of a health care system can be captured by measuring waiting time[11]. For every system, these performance indicators may be different[12], and need to be chosen according to the context.

Performance-based resilience metrics are conventionally designed to assess resilience based on (a) the severity of a disruption (or maximum loss of performance) and (b) the speed of recovery, e.g[12–17].. The underlying assumption is that the more effectively a system restores its performance to acceptable levels after a disruption, the more resilient the system is. Conversely, a lower or more prolonged decline in the performance of a system indicates reduced capacity to manage the disruption. Previous research has mapped different approaches to come to a performance-based resilience metric[6]. The authors distinguish between 6 categories of resilience metrics: based on magnitude (e.g., maximum performance loss[18]), duration (e.g., total duration of disruption[19]), integral (for example, the total performance loss: duration of disruption $\times$ impact[13]), rate (of recovery, or of failure[17,20]), threshold (e.g. continuity of critical functions[21]), and ensemble (a mix of the previous categories, e.g[22]).

While some disruption functions are generic[8], others advocate tailoring the disruption function to the specific hazard and context[10]. For instance, in the context of infectious disease outbreaks, epidemic wave functions have been developed that are fit to disease cases over time[23]. By tailoring the disruption function to the specific contexts, the characteristics of the behaviour of the system can be captured. For instance, while at times it is assumed that infectious diseases follow a normal distribution pattern, empirical data show that asymmetrical behaviour exists, indicating that distributions with non-zero skewness are more appropriate[23]. This can then be captured by using dedicated functions.

To capture the full dynamics of the recovery trajectory for individual crises, disruption approximation functions have been proposed[8]. These disruption functions are generally meant to be fit to (potentially noisy) performance data over time, such that the trajectory and level of resilience of an individual disruption can be identified. While such modelling is useful for isolated events, it falls short in capturing the evolving dynamics of consecutive disruptions that occur in the context of poly-crises.

Measuring adaptation

The resilience cycle, which is commonly used to describe how systems respond to disruptions, is usually defined with 4 different phases: absorption, recovery, adaptation (and sometimes transformation) and preparation or mitigation[24–26]. Adaptation has thus been recognised as a crucial component of resilience science, particularly in social-ecological resilience research, but also increasingly in the engineering resilience context, where the focus is not just on short-term absorption and recovery after a disruption, but on long-term change[27]. From the perspective of the resilience cycle, adapting means to learn from previous events and implementing changes that improve coping with future disruptions (inspired by definitions given in[26,28]). Together with transformation, adaptation is often conceptualized as a capacity to influence the resilience of a system. While adaptation tends to be characterised as a more reactive, transformation is regarded as a proactive mechanism of a change[29–31].

The literature refers to several closely related concepts, such as adaptation, adaptive capacity, and adaptability, which show important distinctions despite their similarities. One distinction is that adaptive capacity[32] and adaptability[33] are often used to describe the potential for change, whereas adaptation refers to observable outcomes[32]. In this context, adaptation can be understood "as a manifestation of adaptive capacity"[32]. Other definitions also exist, putting emphasis on the human dimension, so that adaptability is defined as "the capacity of actors in the system to influence resilience"[27].

Adaptation as a measurable, outcome-based metric also has theoretical roots in learning theory and complex adaptive systems. Essentially, learning is understood as a feedback process[34]: systems facing repeated similar challenges can show learning behaviour, whereby previous experiences influence the performance in the future[35]. This learning manifests as changes in responses (via development of capabilities and capacities) that affect how well systems handle subsequent disruptions. Unlike one-time responses to isolated shocks, adaptation involves cumulative learning that spans multiple disruptions.

Building on social-ecological resilience theory[27,36], we define adaptation as *the capacity of a system to adjust its responses to a disruption over time, resulting in improving (or declining) its performance in responding to successive disruptions*. This definition focuses on performance outcomes, rather than capabilities or capacities, which allows us to measure directly if system performance improves or deteriorates across a sequence of disruptions. The definition explicitly includes the possibility of negative adaptation (i.e., declining performance), which is the situation where the resilience of individual disruptions decreases over successive disruptions.

In contrast to the resilience literature, only a few metrics to measure adaptation have been developed. Most assessment methods and metrics for adaptation can be found in the context of climate change[37]. In this domain, the adaptation metrics are typically used to track progress towards a specific goal (such as the implementation of key policies) of being better prepared for a changing climate[38]. As such, these metrics focus on ex-ante preparedness rather than providing ex-post assessments of a system's performance in response to climate change disruptions.

Adaptation has also been assessed in the healthcare domain. For example, previous research developed an adaptability index to evaluate how non-COVID-19 healthcare in the USA counties responded to two consecutive COVID-19 waves[39]. For this, the authors defined an adaptability index by taking the relative increase in the disruption and recovery rate of two consecutive disruptions. In this way, they conceptualise adaptation as the positive change in dealing with two consecutive disruptions. In case of more than 2 consecutive disruptions, this approach takes the adaptation to be the average adaptation of all pairs of 2 consecutive disruptions. While insightful, this approach narrowed down adaptation to a two-event sequence. However, adaptation and learning clearly unfold over a longer period of time and through multiple disruptions, as exemplified by COVID-19.

This highlights a gap: current methods do not capture the learning dynamics that unfold across *multiple* disruptions. Nowadays, it is not only acknowledged in the social-ecological resilience literature, but also in the engineering resilience literature that adaptation is a crucial part of the resilience cycle. Still, existing measurement approaches treat each disruption independently or average across pairs of events. Thereby, the existing adaptation metrics miss the cumulative dynamic processes across multiple disruptions. Since learning is a continuous process and adaptation unfolds over extended periods, there is a clear need for methodological approaches capable of evaluating long-term adaptation under consecutive disruptions.

We build here on learning theories and model adaptation based on exponential functions. The theoretical and empirical foundations for this choice are provided by organisational psychology and operations research, where learning curves are used to measure how performance improves if organisations or people are repeatedly exposed to similar tasks. The resulting learning curves follow exponential patterns, with rapid initial gains that diminish over time[40]. This pattern reflects the potential processes underlying adaptation: initial learning is steep, but further improvements are increasingly difficult to achieve[41]. The exponential function $f(t) = a \cdot e^{-bt} + c$ captures this dynamic, where b represents the learning rate and c represents the asymptotic performance limit that systems approach through experience. Inspired by theory on learning and forgetting[42], we introduce the concept of adaptation patterns, allowing for modelling periods of adaptation or maladaptation. Periods of adaptation represent learning and adjusting to a disruption, whereas maladaptation represents a pattern of 'forgetting', whereby the disruption results in worse outcomes than for prior disruptions.

In summary, this paper aims to develop a methodology and a corresponding adaptation metric to quantify how a system adapts in response to multiple successive disruptions. Our approach is the first to quantify adaptation by modelling the process using an exponential function. As a result, the proposed approach also allows for a robust quantification of the initial resilience within a sequence of disruptions.

Quantifying adaptation

This section describes the generic approach to measure adaptation in four steps, while in the next section, we showcase how this approach is applied to the COVID-19 case study.

Identify individual disruptions

We start from a system's performance as represented by one or more indicators, which evolve over time. Disruptions are represented as drops in performance. While there may be some overlap between the disruptions in the case of overlapping or compound events, we here assume that the individual disruptions can be identified.

Compute resilience metrics

For each disruption, a resilience metric needs to be computed. The metrics are inspired by resilience measurement theory, see the Background section. To fit different contexts, cases or priorities, our method is metric-agnostic and flexible, meaning that adaptation can be measured using any resilience metric of choice that is relevant to the system. In our case study, we use the Total Performance Loss (TPL) as the metric of interest, as it is a widely used metric that combines both information on the extent of the performance loss, as well as on the duration of the disruption. Other possible metrics that could be applied include maximum performance loss, disruption duration, time to next disruption or recovery speed in case the measurement context calls for this, cf. Fig. 1.

Fit exponential curves

From an adaptation perspective, the focus lies on examining how a given resilience metric evolves over the course of consecutive disruptions. This can be illustrated visually and intuitively by representing each disruption as a point on a two-dimensional plot, where the x-axis denotes the timing of the disruption and the y-axis represents the corresponding performance metric value. Inspired by the theory on learning and adaptation as discussed in the Background section, the following exponential function is fitted to these data points:

$$f(t) = a \cdot e^{-b \cdot t} + c \tag{1}$$

The benefit of this function is that it contains interpretable coefficients to characterise the adaptation, which are used as inputs in the next step. Furthermore, as opposed to a simple linear function, this function is able to model both convex and concave adaptation behaviour, allowing it to capture different learning dynamics over time. Concave adaptive behaviour reveals quick initial adaptation, while convex adaptive behaviour captures delayed learning.

Since real-world systems may not show a single and consistent adaptation behaviour over time, we explore the possibility of multiple adaptation patterns. For example, a system may initially adapt by showing improved response and later maladapt and show deteriorating response, or visa versa. To capture this shift in system behaviour, we allow multiple adaptation patterns rather than the single exponential trend across all disruptions. An adaptation pattern is then a period of consistent improvement (or deterioration) of resilience, with limited instances of deterioration (or improvement). In practice, this means that we fit not one, but multiple exponential curves, in successive order. The best overall fit (the highest R^2 on the combined fit) is chosen. If a fit contains two exponential curves, this indicates a presence of two separate patterns, while a single exponential curve indicates a single adaptation pattern. See Figure 2 for an example.

Since the exponential function contains three parameters, at least three disruptions are required to estimate a single adaptation pattern. Therefore, from three disruptions, one adaptation pattern is possible, while from six disruptions, two adaptation patterns are possible, etc.

For systems with more than 6 disruptions, the breakpoint where the first adaptation pattern ends and the second adaptation pattern begins needs to be determined. In case of 7 disruptions, like the example in Fig. 2, break-off points are possible between disruptions three and four, or between four and five. In such a case, the best overall fit determines the placement of the break-off point.

Exponential coefficients as adaptation metric

In equation 1, *b* is the rate of change. For positive values of *a*, positive values of *b* mean adaptation, while negative values mean maladaptation. For negative values of *a*, this interpretation reverses. Therefore, the final adaptation metric α is equal to *b* multiplied by the sign of *a*. Thus, positive numbers of α mean adaptation, and negative number mean maladaptation. Therefore α represents the *learning rate* in our proposed adaptation metric.

$$\alpha = sgn(a) \cdot b \tag{2}$$

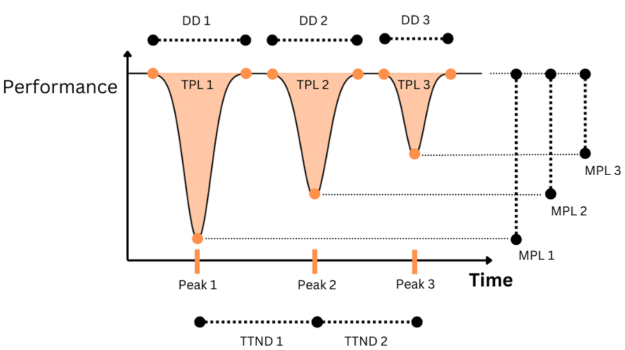

Fig. 1. The performance over time of a system X under three consecutive disruptions. Given that individual disruptions are identifiable, performance metrics for each single disruption can be computed. In this case, we show the following: MPL = Maximum Performance Loss, TPL = Total Performance Loss, DD = Disruption Duration, TTND = Time to next Disruption.

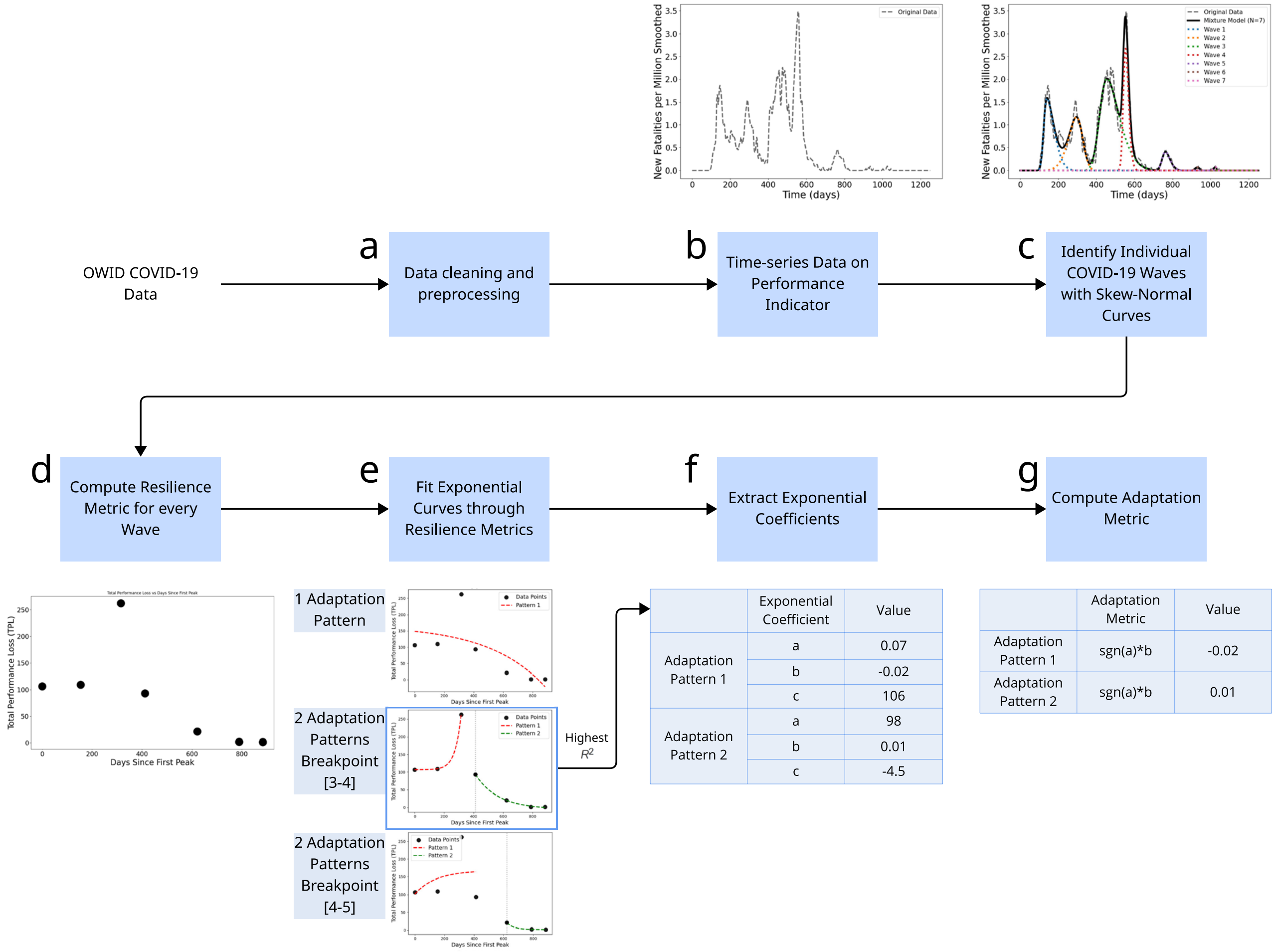

Fig. 2. Step-by-step illustration of the methodology. It depicts the steps taken in the proposed approach for quantifying adaptation (but applied to an example country (Kuwait) from the case study).

COVID-19 case study: measuring adaptation of 180 countries and territories

In this section, we first describe the data and how it is preprocessed. Then, we go into detail on how we applied the approach for quantifying adaptation to the case study. This process can be broken down into 5 subprocesses: 1) identifying individual COVID-19 waves by skew-normal curve fitting, 2) computing performance metrics of every individual COVID-19 wave, 3) fitting exponential curves to these performance metrics, 4) extracting the function's coefficients and 5) computing the adaptation metric. Figure 2 provides a conceptual overview of the methods and where these are discussed.

The COVID-19 pandemic was selected as a case study due to its consecutive waves and the varying levels of adaptation across countries. The COVID-19 case provides a suitable setting for demonstrating our approach to quantifying adaptation, particularly because national adaptation levels of countries were not fully understood.

Data

Since it is one of the important public health objectives of countries to prevent avoidable mortality due to disease, the key performance indicator used in this study is the number of COVID-19 fatalities per million inhabitants. Data on COVID-19 fatalities over time is available at Our World in Data for 219 countries and territories[43,44]. Data is available for some countries starting from January 1 st 2020, and for some countries ending on June 18th 2023 (data collection date). The time interval for which data was available for all countries is January 8th 2020 to June 14th 2023, therefore our analysis is done on this time interval.

In the next step, we apply 7-day smoothing to daily new fatalities per million inhabitants to reduce the noise resulting from high variability in small countries (see step a in Fig. 2). This helps in a later step, where we fit a mixture of skew-normal curves. For some low-population countries it is difficult to identify a COVID-19 wave due to very noisy data, so we exclude countries with a population of less than 50.000, eliminating 15 countries and territories from further steps.

To compare several adaptation groups, we examine whether differences between groups can be identified based on country-level statistics related to the health system. Our World in Data also has descriptive statistics available from the same aforementioned data set.

Applying the approach for quantifying adaptation step by step

In this section, we walk through the same steps as described in the previous section on quantifying adaptation, but here we discuss the details of applying this to the case study.

Identifying individual COVID-19 waves by fitting a mixture of skew-normal curves

Identifying the different COVID-19 waves is done by fitting a mixture of skew-normal curves to the temporal fatality data for every country, as shown in step c in Fig. 2. A skew-normal distribution is normally used as a probability distribution that generalises the normal distribution to allow for non-zero skewness. In this case, we use this distribution to approximate a wave of COVID-19 fatalities, to allow for epidemic waves where the increase and decrease rates are not the same. In order to do this, the distribution is multiplied by a weight, a parameter that is fitted together with the distributions' parameters. A single curve or wave $C(t)$ can be described by the skew-normal function F taking the location parameter ξ, a scale parameter ω and a shape parameter α and multiplied by a weight parameter w (see Equation 3). The curve provides an overall temporal pattern of COVID-19 fatalities in a country, specifically determining when waves happened and with which intensity.

$$C(t) = w \cdot F_{\xi,\omega,\alpha}(t) \tag{3}$$

Now, the mixture of curves to approximate the total trajectory $T(t)$ is described as summing the n curves together.

$$T(t) = \sum_{i=1}^{n} C_i(t) \tag{4}$$

An important step here is to determine n, the number of curves that each trajectory consists of. The objective is to approximate the empirical data well, while avoiding overfitting to short-term fluctuations or noise. This is why we chose to determine n as follows. First, we fit a range of ten different mixtures from two to eleven curves, using the Trust Region Reflective optimisation algorithm that minimises the residual sum of squares. Then, the R^2 value is computed for every mixture to determine the goodness of fit. The mixture with the highest R^2 value is the best fit, but visual inspection shows that this leads to overfitting to noise. Therefore, we choose the mixture with the smallest number of n, but within a 0.01 range of the maximum R^2 value across all candidate mixtures. We validated this method by systematic visual inspection across countries and comparing our approach to: 1) taking the n for which R^2 is the maximum (the maximizing method), and 2) taking the lowest n for which the R^2 does not improve significantly any more (the plateauing method).

Across various cases, our method consistently produced the most interpretable and realistic wave decomposition, when compared to the two alternatives, resulting in a median R^2 value of 0.9583, and 86% of the countries having R^2 values higher than 0.90.

The expectation could be that for countries with less waves, the fitting process is easier, resulting in good fits being more likely. However, even for countries with six or more, the median R^2 value remains high at 0.9495 which indicates robust performance.

Since this method might result in having consecutive waves that overlap significantly in some countries, we explicitly measure the extent of this overlap. For each pair of consecutive waves C_1 and C_2 we computed the Intersection over Union (IoU) metric (see Supplementary Material S1), which reveals the proportion of shared area relative to the total area covered by both waves. These IoU values are used to identify the cases where two waves cannot be separated. Countries that have at least one pair of consecutive waves with an IoU score larger than 0.4 (40% overlap) are removed from further analysis. This results in 5 countries being removed.

Computing resilience metrics

Next, the Total Performance Loss (TPL) is computed for every COVID-19 wave, as visually displayed in Fig. 2 at step d for the examples of 3 pandemic waves. TPL is computed as the total area under each fitted wave.

Fitting exponential curves through resilience metrics

In order to fit the exponential curve (1) to the resilience metrics over time, we take the position in time of each wave to be the time that the highest point of the (fitted) wave occurred. To make the comparison easy, we shift these times such that the first wave is set to begin at time 0, and all other waves are shifted on the x-axis accordingly. So, if the highest point of wave 1 occurs on day 50, every wave time is subtracted by 50 (see step d in Fig. 2).

Now that we have the resilience metric and time placement for each wave, we can fit an exponential function for each country to determine whether a clear pattern of adaptation emerges, which is visually depicted in step e in Figure 2. Fitting is performed using the Levenberg-Marquardt algorithm, minimising the residual sum of squares. For countries with less than 3 waves (and thus less than 3 data points) identified in the skew-normal fitting step, it is not possible to fit the exponential equation, since the exponential equation consists of 3 parameters. We disregard these 19 countries from further analysis. Thus, for 180 countries, we can now compute the adaptation metrics. Figure S3 and Table S4 in the Supplementary Material give an overview of how well the exponential functions fit (in R^2) for individual countries. It can be seen that for some countries, the R^2 is quite low.

Exponential coefficients as adaptation metric
Since the exponential curves model the general adaptation behaviour of a single country for a specific performance metric, we take the curve coefficients as metrics for adaptation (step f and g in Fig. 2). Here, as discussed in the previous section, we take b and $sgn(a)$ to compute the adaptation metric.

Adaptation profiles of countries
Having fitted the exponential curve(s) for every country, we categorize countries based on the number and direction of the adaptation patterns they exhibit. An adaptation pattern is defined as a period of which the fitted exponential function shows a consistent adaptation behaviour indicated by the sign of the adaptation metric. Since the maximum number of disruptions in our data is 11, a country can exhibit at most three adaptation patterns. This means that there are three primary profiles: countries with one, two or three adaptation patterns. Within these profiles, we create categories based on adaptation behaviour: adaptation or maladaptation. The first profile includes countries with a single adaptation pattern. Within this profile, there are two categories; one with a positive adaptation metric α, and one with negative α, representing adaptation and maladaptation, respectively.

The second profile includes countries with two adaptation patterns, where the sign again determines four distinctive adaptation trajectories: adapt-adapt, adapt-maladapt, maladapt-adapt and maladapt-maladapt. Countries with three adaptation patterns form the third profile due to the small number of such cases (i.e. 8 countries). To avoid excessive fragmentation, we do not further subdivide this group. This profiling and categorization yield a set of mutually exclusive adaptation trajectory types for all countries.

Results

To understand the behaviour associated with the adaptation patterns, we plot the raw COVID-19 fatality time-series data of countries that correspond to each category separately in Fig. 3. The median and interquartile range are included as well. This visualization allows us to examine the temporal evolution of COVID-19 responses.

To compare countries with different mortality levels, we normalize each country's time series data such that its maximum fatality value equals 1. Since the timing and duration of the pandemic vary across countries (i.e., occurrence of the first and last disruption), the time axis is rescaled such that the peak of the first identified disruption is set to 0, and the time of the last disruption is set to 1. This normalization enables comparison of the relative progression of fatalities throughout the pandemic and, therefore, highlights the adaptation dynamics associated with each profile.

On the world map (Fig. 3h), adaptation profiles appear to be spatially dispersed. For the profiles with a single adaptation pattern, a clear difference in the trend of fatalities over time can be observed. Specifically, the profiles categorized as "adapt" (Fig. 3a) tend to show a decrease in fatalities over time, while the "maladapt" (b) profile shows an increasing trend. For the countries with 3 adaptation patterns (g), no clear trend is observed, since these patterns do not have the same adaptation direction.

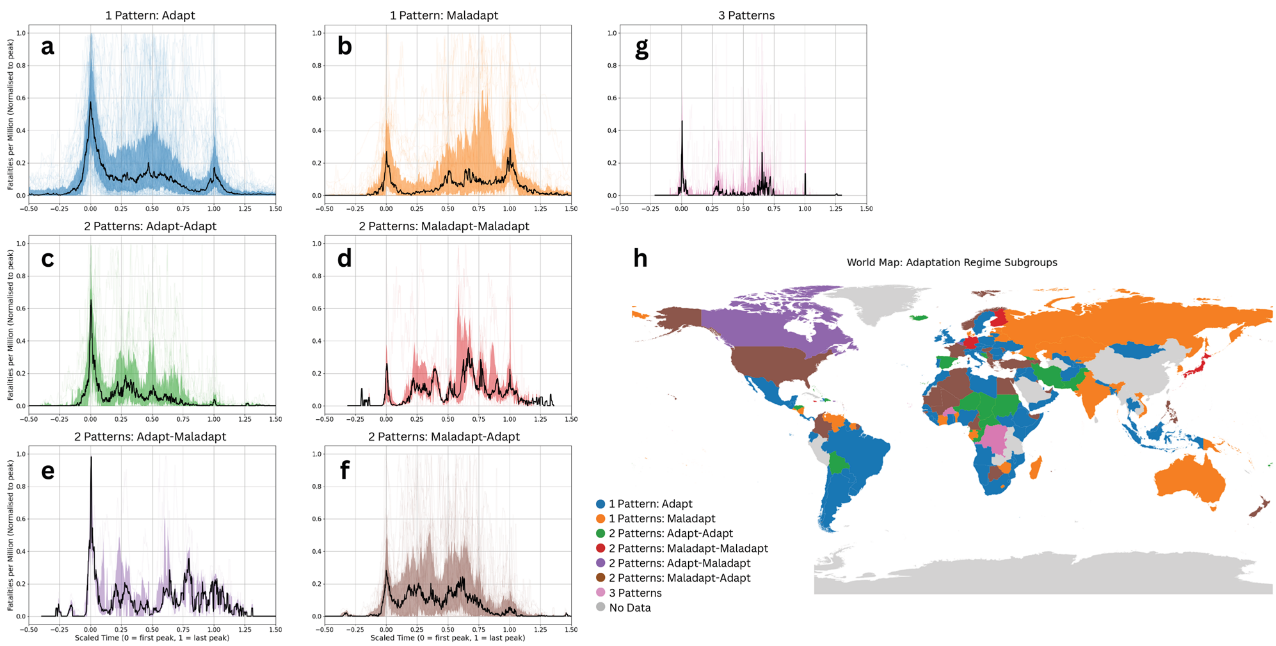

Fig. 3. For each subgroup of countries, the COVID-19 fatalities over time (normalised) are plotted, including a subgroup median (black line) and interquartile range (filled area). For each country, time 0 is the time of the modelled peak of the country's first wave, and time 1 is the peak of the last wave. The countries included in each cluster are plotted on a world map (colour-coded).

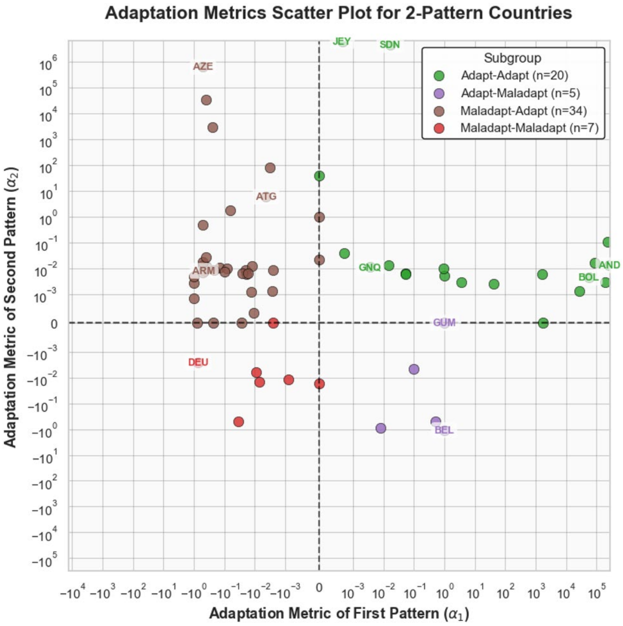

Fig. 4. For the countries with two adaptation patterns, the value of the adaptation metric of the first and second pattern are plotted.

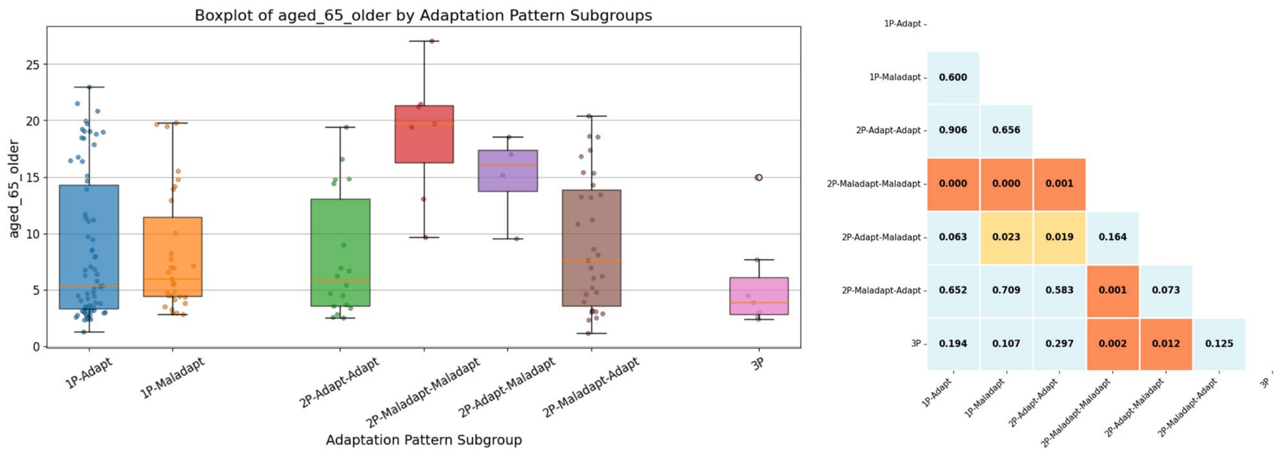

Fig. 5. Boxplots of the percentage of population older than 65, split out over the adaptation pattern profiles, with on the right a table with p-values of the two-sided Mann-Whitney U statistical test between the groups.

The four subgroups in the profile with two adaptation patterns, also exhibit behaviour that can be linked back to their subgroup association. It can be observed that the two groups that adapt in the second pattern (c and f) tend to have relatively lower COVID fatalities towards the end of the pandemic. This trend is less obvious in the other two subgroups (d and e). For the two subgroups that adapt in the first pattern (c and e), we can see relatively higher peaks at the beginning followed by decline, which is consistent with adaptation occurring in the first pattern. The other groups, with maladaptation as a first pattern (d and f), do not exhibit evidence of this behaviour.

When the adaptation metrics of the first and second patterns are plotted for every country (see Fig. 4), it is evident that most countries tended to adapt during the second pattern. Out of 66 countries, only twelve are characterized as maladapting in the second pattern. Remarkably, most countries show maladaptation in the first pattern, while the majority shows the signs of adaptation in the second pattern.

To investigate whether the social-demographic factors explain the adaptation patterns, we used country statistics and plotted the distributions of the percentage elderly population and population density, in Figs. 5 and 6. The percentage of people aged 65+ of the two profiles that end the pandemic in a maladapting pattern (adapt-maladapt and maladapt-maladapt) are significantly higher. For the population density, the maladapt-maladapt subgroup stands out, having a significantly higher population density. The adapt-adapt profile shows a significantly lower population density. For both variables, not many significant differences were found

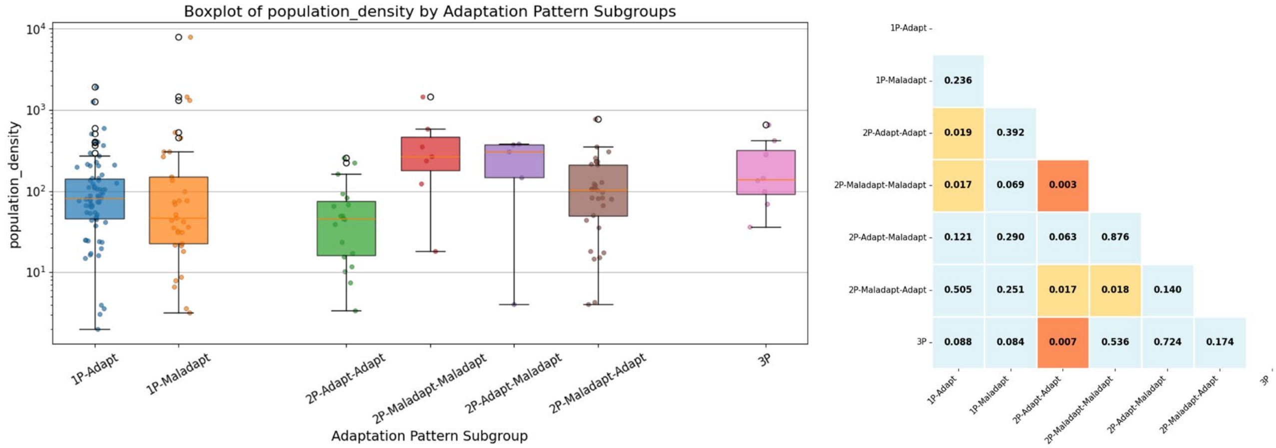

Fig. 6. Boxplots of the population density, split out over the adaptation pattern profiles, with on the right a table with p-values of the two-sided Mann-Whitney U statistical test between the groups.

among other profiles, such as between those with a single adaptation pattern (i.e., adapt and maladapt). Based on previous research, both variables are considered relevant for total fatality, since the elderly population was particularly vulnerable, and population density has been identified as one of the key determinants in the spread of disease[45,46]. Therefore, it is surprising that there seems to be a correlation to the adaptation capacity as well. The potential mechanisms through which this may happen may be numerous, and are suitable topics for further research.

The adaptation categories are spatially dispersed on the world map (Fig. 3h), with subgroups being present in several continents. This is different from research where countries are clustered based on fatalities temporal behaviour[47,48]. For example, research that performed country-wise hierarchical clustering on COVID-19 fatality data found clusters that, to a large extent, follow similarity in distance as well, meaning that clusters were often present in the same continents[48]. They also found that this clustering may be explained by the difference in percentage of population above 65 years of age.

Discussion

Our study focuses on adaptation patterns to differentiate between improvement or deterioration in responses across successive waves of disruptions. Even though especially for COVID-19 there is a substantial body of literature on the evolution of COVID-19 fatalities over time, most of these studies focused on clustering countries based on similarities in observed time series data[47–49]. In contrast, our study quantifies adaptation as a dynamic process of learning and unlearning that evolves across successive disruptions.

The proposed approach identifies whether performance improves or deteriorates over time by fitting exponential functions to a sequence of resilience metrics. The proposed approach using the exponential function captures the non-linear nature of adaptation. Concave curves are characterized by rapid initial adaptation followed by decline, and convex adaptation curves represent delayed learning where adaptive behaviour increases in the later stages.

Furthermore, the proposed approach allows for multiple adaptation patterns for each system. In this way, we can track changes of the adaptation behaviour itself. Rather than assuming a uniform adaptation trend across all disruptions, the approach identifies temporally bounded phases in which adaptation behaviour is similar, while still allowing for transition between these phases. By doing so, patterns such as early maladaptation followed by later improvements to adaptation or initial adaptation that diminishes over time, leading to maladaptation, can be captured by our approach. These adaptation patterns offer an in-depth analysis of when systems learn, delay learning, or fail to adapt.

This methodological flexibility enables the method to represent a wide range of real-world adaptive behaviours that involve delayed learning, which could be due to institutional inertia, policy changes, or other socio-spatial constraints. While the proposed approach captures temporal patterns that are consistent with learning and unlearning, it is not intended to reveal causal relationships between adaptation trajectories and specific policies, institutional arrangements, or socio-spatial factors. Rather, the method provides a systematic way of identifying and comparing adaptation dynamics, which can then serve as a basis for subsequent causal or explanatory analysis.

Adaptation measured in this study is a purely quantitative measure that relies on the selected metric rather than a normative measure. This means that specific adaptations may vary and involve trade-offs. For example, adaptation in one domain (in our case, measured by COVID-19 fatalities) may lead to maladaptation in another, as it may come at the expense of social equity, political stability, and other important considerations. Therefore, it is essential to acknowledge that our approach captures adaptation through a single performance metric lens, while adaptation is inherently multidimensional across social, economic, and ecological domains. Consequently, any single metric will provide only a partial view. Different performance indicators will reveal different adaptation trajectories, potentially leading to contradictions among them. The result is not a complete picture of adaptation; rather, it is a cross-section of a complex phenomenon. Nevertheless, our approach provides an analytical, systematic, and reproducible method for quantifying and observing adaptation dynamics over time.

Although we illustrated this approach using COVID-19 data, it is not pandemic-specific. COVID-19 is a suitable case as it involves successive disruptions over time and presents a measurable performance indicator. However, the method can be applied to any system experiencing successive disruptions, provided that system performance can be quantified. Examples include infrastructure systems that are exposed to consecutive natural hazards, operational shocks due to attacks, etc. The proposed method offers systematic insights into the adaptation dynamics across a wide range of domains.

One limitation of our proposed approach is that the exponential function used to model the adaptation behaviour does not always provide a strong fit to the resilience metrics. For 30.8% of countries, the R^2 is less than 0.5 (see Supplementary Material S2) indicating that in some cases, adaptive behaviour is not monotonic. Therefore, the goodness of fit itself may be interpreted as an informative indicator of (non-)smoothness or stability of adaptation behaviour, rather than solely as a measure of model performance. However, it must be noted that the assumption of exponential learning may hold less for different types of successive disruptions, underlining the potential for tailoring this function to specific contexts. Moreover, the exponential fits depend on previous steps, such as how the disruptions are identified. If the disruption identification approach is adjusted such that fewer or more disruptions are identified, this alters the fitting of the exponential function and the resulting adaptation metric.

Another methodological limitation stems from the parametric nature of the exponential function, which requires a minimum of three disruptions to estimate its parameters (a, b, and c) for assessing adaptation. As a result, systems experiencing only two successive disruptions cannot be analyzed using the proposed approach, which leads to the exclusion of countries like China, which had only two COVID-19 waves.

While this case study did not go into detail to the role of exponential parameters a and c, $a + c$ determines the value of the function at $t = 0$. Therefore, $a + c$ is an assessment of resilience at the beginning of the successive disruption event. This could be used in future work as a robust estimate for the resilience value in the the beginning of a long-term crisis. Other future work could include a multi-metric approach. Since it is known that some resilience metrics may also be conflicting, applying our method with multiple resilience metrics at the same time might further the understanding of the potential trade-offs between these resilience metrics in the long-term.

A case-study-specific limitation is the quality and consistency of COVID-19 fatality data. To identify individual disruptions, we fitted skew-normal curves to the COVID-19 fatality data over time. In some cases, this resulted in suboptimal fits. Our adaptation results depend on how well we can identify individual COVID-19 waves, and improving this step would likely lead to robust adaptation estimates. However, it is possible that skew-normal curves will sometimes remain challenging to fit despite better fitting methods, due to the fact that COVID-19 data is not always reliable. Therefore, differences and inconsistencies between the fitted waves and observed trajectories do not necessarily indicate the failure of our approach but may be due to heterogeneous data reporting, differences in data collection, and the absence of a unified reporting protocol. Nevertheless, some degree of uncertainty may remain inherent in such empirical pandemic data.

Conclusion

In this paper, we introduced a novel approach for quantifying the adaptation of systems to successive disruptions. Since the response to successive disruptions cannot be disentangled from each other, adaptation becomes a crucial part of successive event resilience. Our proposed approach uses an exponential equation, of which the coefficients give insight into a system's adaptation behaviour. Like the recovery rate quantifies the speed of recovery after a single disruption, our proposed adaptation metric quantifies changes over the course of multiple consecutive disruptions. Thus, it indicates the adaptation or learning of a system over a long period of time known as an adaptation pattern.

The contribution of this paper is twofold. First, by building on the existing resilience measurements that focus on single disruptions, the proposed approach introduced a means to quantify adaptation, and therefore, offers a deeper understanding of long-term behaviour. Second, the COVID-19 case study showcases the application of the approach and provides empirical insight into adaptation profiles exhibited by countries. The resulting profiles show different behaviours based on the direction of adaptation patterns. This gives crucial insight into the adaptation pathways of individual systems over the course of multiple successive disruptions.

The approach is general in two ways. First, it can be applied to any successive disruption event for which a performance indicator exists. Secondly, it is not restricted to the resilience metric used in this paper (TPL), but can be applied to any of the numerous existing resilience metrics that can be computed from individual disruptions.

In the case study, we have chosen to select COVID-19 fatalities as a performance indicator. However, this kind of disruption is typically not represented by just one (healthcare outcome) performance dimension. In future work, other dimensions like economic, social, and policy indicators also need to be taken into consideration when doing a comprehensive adaptation assessment. The extension of the proposed adaptation methodology to multiple performance indicators would have the potential to identify observed trade-offs between different indicators. Next to relating adaptation to these dynamic indicators, future work could also relate static or slowly changing variables of systems to the degree of adaptation.

Data availability

The datasets generated and/or analysed during the current study are available in the Github repository, https://github.com/fvsteijn/Adaptation-Metric.git.

Received: 14 July 2025; Accepted: 6 May 2026
Published online: 30 May 2026

References

1. Eisenberg, D. A., Seager, T. P. & Alderson, D. L. The rebound curve is a poor model of resilience. *PNAS Nexus* **4**, 052. https://doi.org/10.1093/pnasnexus/pgaf052 (2025).
2. Woods, D. D. The theory of graceful extensibility: Basic rules that govern adaptive systems. *Environ. Syst. Decis.* **38**, 433–457. https://doi.org/10.1007/s10669-018-9708-3 (2018).
3. Folke, C. et al. Resilience thinking: integrating resilience, adaptability and transformability. *Ecology and society* **15**, (2010).
4. Jones, L., Constas, A., Matthews, N. & Verkaart, S. Advancing resilience measurement. *Nat. Sustain.* **4**, 288–289. https://doi.org/10.1038/s41893-020-00642-x (2021).
5. Feldmeyer, D., Nowak, W., Jamshed, A. & Birkmann, J. An open resilience index: Crowdsourced indicators empirically developed from natural hazard and climatic event data. *Sci. Total Environ.* **774**, 145734. https://doi.org/10.1016/j.scitotenv.2021.145734 (2021).
6. Poulin, C. & Kane, M. B. Infrastructure resilience curves: Performance measures and summary metrics. *Reliab. Eng. Syst. Saf.* **216**, 107926. https://doi.org/10.1016/j.ress.2021.107926 (2021).
7. Woods, D. D. Four concepts for resilience and the implications for the future of resilience engineering. *Reliab. Eng. Syst. Saf.* **141**, 5–9. https://doi.org/10.1016/j.ress.2015.03.018 (2015).
8. Cassottana, B., Aydin, N. Y. & Tang, L. C. Quantitative assessment of system response during disruptions: An application to water distribution systems. *J. Water Resour. Plan. Manag.* **147**, 04021002. https://doi.org/10.1061/(ASCE)WR.1943-5452.0001334 (2021).
9. Aydin, N. Y. Measuring topological and operational resilience and recovery of water networks for planning and management. In *World Environmental and Water Resources Congress 2018*, 370–379 (American Society of Civil Engineers Reston, VA, 2018).
10. Yabe, T., Rao, P. & Ukkusuri, S. V. Resilience of interdependent urban socio-physical systems using large-scale mobility data: Modeling recovery dynamics. *Sustain. Cities Soc.* **75**, 103237. https://doi.org/10.1016/j.scs.2021.103237 (2021).
11. Cimellaro, G. P., Reinhorn, A. M. & Bruneau, M. Seismic resilience of a hospital system. *Struct. Infrastruct. Eng.* **6**, 127–144. https://doi.org/10.1080/15732470802663847 (2010).
12. Tang, J., Han, S., Wang, J., He, B. & Peng, J. A comparative analysis of performance-based resilience metrics via a quantitative-qualitative combined approach: Are we measuring the same thing?. *Int. J. Disaster Risk Sci.* **14**, 736–750. https://doi.org/10.1007/s13753-023-00519-5 (2023).
13. Bruneau, M. et al. A framework to quantitatively assess and enhance the seismic resilience of communities. *Earthq. Spectra.* **19**, 733–752. https://doi.org/10.1193/1.1623497 (2003).
14. Platt, S., Brown, D. & Hughes, M. Measuring resilience and recovery. *Int. J. Disaster Risk Reduct.* **19**, 447–460. https://doi.org/10.1016/j.ijdrr.2016.05.006 (2016).
15. Hosseini, S., Barker, K. & Ramirez-Marquez, J. E. A review of definitions and measures of system resilience. *Reliab. Eng. Syst. Saf.* **145**, 47–61. https://doi.org/10.1016/j.ress.2015.08.006 (2016).
16. Shen, L., Cassottana, B., Heinimann, H. R. & Tang, L. C. Large-scale systems resilience: A survey and unifying framework. *Qual. Reliab. Eng. Int.* **36**, 1386–1401. https://doi.org/10.1002/qre.2634 (2020).
17. Aydin, N. Y., Duzgun, H. S., Heinimann, H. R., Wenzel, F. & Gnyawali, K. R. Framework for improving the resilience and recovery of transportation networks under geohazard risks. *Int. J. Disaster Risk Reduct.* **31**, 832–843. https://doi.org/10.1016/j.ijdrr.2018.07.022 (2018).
18. Cassottana, B., Shen, L. & Tang, L. C. Modeling the recovery process: A key dimension of resilience. *Reliab. Eng. Syst. Saf.* **190**, 106528. https://doi.org/10.1016/j.ress.2019.106528 (2019).
19. Zobel, C. W. Representing perceived tradeoffs in defining disaster resilience. *Decis. Support Syst.* **50**, 394–403. https://doi.org/10.1016/j.dss.2010.10.001 (2011).
20. Cassottana, B., Balakrishnan, S., Aydin, N. Y. & Sansavini, G. Designing resilient and economically viable water distribution systems: A multi-dimensional approach. *Resilient Cities Struct.* **2**, 19–29 (2023).
21. Chang, S. E. & Shinozuka, M. Measuring improvements in the disaster resilience of communities. *Earthq. Spectra.* **20**, 739–755 (2004).
22. Najafi, J., Peiravi, A. & Guerrero, J. M. Power distribution system improvement planning under hurricanes based on a new resilience index. *Sustain. Cities Soc.* **39**, 592–604 (2018).
23. Ćmiel, A. M., & Ćmiel, B. A simple method to describe the COVID-19 trajectory and dynamics in any country based on Johnson cumulative density function fitting. *Sci. Rep.* **11**, 17744. https://doi.org/10.1038/s41598-021-97285-5 (2021).
24. Connelly, E. B. et al. Features of resilience. *Environ. Syst. Decis.* **37**, 46–50. https://doi.org/10.1007/s10669-017-9634-9 (2017).
25. Rehak, D., Senovsky, P. & Slivkova, S. Resilience of critical infrastructure elements and its main factors. *Systems* **6**(2), 21. https://doi.org/10.3390/systems6020021 (2018).
26. Mentges, A., Halekotte, L., Schneider, M., Demmer, T. & Lichte, D. A resilience glossary shaped by context: Reviewing resilience-related terms for critical infrastructures. *Int. J. Disaster Risk Reduct.* **96**, 103893. https://doi.org/10.1016/j.ijdrr.2023.103893 (2023).
27. Walker, B., Holling, C. S., Carpenter, S. R. & Kinzig, A. Resilience, Adaptability and Transformability in Social–ecological Systems. *Ecology and Society* **9**, (2004). Publisher: Resilience Alliance Inc.
28. Sharifi, A. & Yamagata, Y. Principles and criteria for assessing urban energy resilience: A literature review. *Renew. Sustain. Energy Rev.* **60**, 1654–1677. https://doi.org/10.1016/j.rser.2016.03.028 (2016).
29. Elmqvist, T. et al. Sustainability and resilience for transformation in the urban century. *Nat. Sustain.* **2**, 267–273. https://doi.org/10.1038/s41893-019-0250-1 (2019).
30. Folke, C. et al. Resilience thinking: Integrating resilience, adaptability and transformability. *Ecol. Soc.* **15**, art20. https://doi.org/10.5751/ES-03610-150420 (2010).
31. Holling, C. S. Resilience and stability of ecological systems. *Annu. Rev. Ecol. Syst.* https://doi.org/10.1146/annurev.es.04.110173.000245 (1973).
32. Smit, B. & Wandel, J. Adaptation, adaptive capacity and vulnerability. *Glob. Environ. Change.* **16**, 282–292. https://doi.org/10.1016/j.gloenvcha.2006.03.008 (2006).
33. Berkeley, A. R., Wallace, M. & Coo, C. A framework for establishing critical infrastructure resilience goals. *Final report and recommendations by the council, national infrastructure advisory council* **26**, (2010).
34. Sterman, J. D. Learning in and about complex systems. *Syst. Dyn. Rev.* **10**, 291–330 (1994).
35. Duffield, S. & Whitty, S. J. Developing a systemic lessons learned knowledge model for organisational learning through projects. *Int. J. Proj. Manag.* **33**, 311–324 (2015).
36. Folke, C. Resilience: The emergence of a perspective for social–ecological systems analyses. *Glob. Environ. Change* **16**, 253–267. https://doi.org/10.1016/j.gloenvcha.2006.04.002 (2006).
37. Goonesekera, S. M. & Olazabal, M. Climate adaptation indicators and metrics: State of local policy practice. *Ecol. Indic.* **145**, 109657. https://doi.org/10.1016/j.ecolind.2022.109657 (2022).
38. Hale, T. N. et al. Sub- and non-state climate action: a framework to assess progress, implementation and impact. *Climate Policy* **21**, 406–420. https://doi.org/10.1080/14693062.2020.1828796 (2021).

39. Zhong, L., Lopez, D., Pei, S. & Gao, J. Healthcare system resilience and adaptability to pandemic disruptions in the United States. *Nat. Med.* **30**, 2311–2319. https://doi.org/10.1038/s41591-024-03103-6 (2024).
40. Yelle, L. E. The learning curve: Historical review and comprehensive survey. *Decis. Sci.* **10**, 302–328 (1979).
41. Epple, D., Argote, L. & Murphy, K. An empirical investigation of the microstructure of knowledge acquisition and transfer through learning by doing. *Oper. Res.* **44**, 77–86 (1996).
42. Benkard, C. L. Learning and forgetting: The dynamics of aircraft production. *Am. Econ. Rev.* **90**, 1034–1054 (2000).
43. Mathieu, E. et al. Coronavirus pandemic (covid-19). *Our World in Data* (2020). Https://ourworldindata.org/coronavirus.
44. Data on COVID-19 (coronavirus) by Our World in Data. https://github.com/owid/covid-19-data. Accessed: 2023-08-29.
45. Chang, D., Chang, X., He, Y. & Tan, K. J. K. The determinants of COVID-19 morbidity and mortality across countries. *Sci. Rep.* **12**, 5888 (2022).
46. Martins-Filho, P. R. Relationship between population density and COVID-19 incidence and mortality estimates: A county-level analysis. *J. Infect. Public Health.* **14**, 1087 (2021).
47. Gohari, K., Kazemnejad, A., Sheidaei, A. & Hajari, S. Clustering of countries according to the COVID-19 incidence and mortality rates. *BMC Public Health* https://doi.org/10.1186/s12889-022-13086-z (2022).
48. Luo, Z., Zhang, L., Liu, N. & Wu, Y. Time series clustering of COVID-19 pandemic-related data. *Data Sci. Manag.* **6**, 79–87. https://doi.org/10.1016/j.dsm.2023.03.003 (2023).
49. Bucci, A., Ippoliti, L., Valentini, P. & Fontanella, S. Clustering spatio-temporal series of confirmed COVID-19 deaths in Europe. *Spat. Stat.* **49**, 100543 (2022).

Author contributions

F.v.S.: conceptualisation, methodology, visualisations, writing - original draft, writing - review & editing. N.Y.A.: conceptualisation, methodology, writing - review & editing, supervision. N.D.: conceptualisation, methodology, review & editing, supervision. T.C.: conceptualisation, methodology, writing - review & editing, supervision.

Declarations

Competing interests

The authors declare no competing interests.

Additional information

Supplementary Information The online version contains supplementary material available at https://doi.org/10.1038/s41598-026-52678-2.

Correspondence and requests for materials should be addressed to F.S.

Reprints and permissions information is available at www.nature.com/reprints.

Publisher's note Springer Nature remains neutral with regard to jurisdictional claims in published maps and institutional affiliations.